Aerosol direct shortwave radiative forcing effect based on SBDART model in the Pearl River Delta, Guangdong (China)

Lili Li

State Key Laboratory of Organic Geochemistry,
Guangzhou Institute of Geochemistry,
Chinese Academy of Sciences,
Guangzhou 510640, China
Email: lilili@gig.ac.cn
and
Graduate University of Chinese Academy of Sciences,
Beijing 100049, China

Yunpeng Wang*

State Key Laboratory of Organic Geochemistry,
Guangzhou Institute of Geochemistry,
Chinese Academy of Sciences,
Guangzhou 510640, China
Fax: +86-20-85290197
Email: wangyp@gig.ac.cn
*Corresponding author

Abstract: Aerosols play an important role in the energy budget of the earth-atmosphere system. In this paper, we studied aerosol shortwave direct radiative forcing (DRF) effects in Pearl River Delta based on SBDART and a 'two-layer-single-wavelength' model. Simulation results indicated that the underlying surface type and solar zenith angle have significant impacts on aerosol radiative forcing. The comparison between aerosol radiative forcing effects on urban asphalt surface and vegetation shows cooling and warming effects of aerosol shortwave radiative forcing on urban asphalt are much more apparent than that on vegetation, implying aerosols over asphalt-predominated cities will impact the local climate. Then we estimated variations of average DRF and net radiation flux with solar zenith angle in the Pearl River Delta. DRF indicates warming at solar zenith angles of 0°, 20°, 40° and 60°, but cooling at 80°. Net radiation flux increases with a decrease in aerosol optical thickness (AOT) at low elevation, but with an increase in AOT above 5 km.

Keywords: aerosols; shortwave direct radiative forcing; net flux; underlying surface; solar zenith angle; Santa Barbara DISORT atmospheric radiative transfer; SBDART; Pearl River Delta; China.

Reference to this paper should be made as follows: Li, L. and Wang, Y. (2017) 'Aerosol direct shortwave radiative forcing effect based on SBDART model in the Pearl River Delta, Guangdong (China)', *Int. J. Global Warming*, Vol. 13, No. 1, pp.1–15.

Biographical notes: Lili Li received her BS in Geographic Information System in Central South University, Changsha, China in 2010, and her MS and PhD degrees in Environment Science from the Guangzhou Institute of Geochemistry, Chinese Academy of Sciences (GIGCAS), Guangzhou, China, in 2015. She is now a Research Assistant in (GIGCAS), and her main research interests are atmospheric remote sensing, air quality observation and simulation.

Yunpeng Wang received his BS in Geology from Lanzhou University, Lanzhou, China, in 1990, and his MS and PhD degrees in Remote Sensing and Geochemistry from the Guangzhou Institute of Geochemistry, Chinese Academy of Sciences (GIGCAS), Guangzhou, China, in 1992 and 1996, respectively. He has been with GIGCAS since 1996, where he has been a Research Professor since 2002. His main research interests are remote sensing and applications on environment, geology and geochemistry.

1 Introduction

Aerosols are fine particles that are suspended in air as liquid or solid, and observed as dust, smoke and haze, significantly influencing global climatic changes and regional environment (IPCC, 2007). Tropospheric aerosols directly affect the radiative balance and climate on the earth through scattering and absorbing solar radiation (Li et al., 2007; Myhre et al., 1998; Penner et al., 1994; Twomey, 1974). They also impose an indirect effect by modifying the cloud albedo (Albrecht, 1989) and the cloud lifetime (Pincus and Baker, 1994) as cloud condensation nuclei (Carlson et al., 1995; Kaufman and Fraser, 1997; Kaufman and Koren, 2006).

Advances have been made in recent years on the study of aerosol radiative forcing and its impact on climate across the world (Alam et al., 2011; El-Metwally et al., 2011; Gao et al., 2003; Kim et al., 2010; Lau and Kim, 2006; Reddy et al., 2004; Wu, 2003; Zhang et al., 2012). Models have been applied to evaluate the direct radiative forcing (DRF) for anthropogenic aerosol species. The global annual average radiative forcing is estimated as –0.4W/m^2 (–0.2–0.8 W/m^2) for sulphate aerosols (Alam et al., 2011; Hobbs et al., 1997; Ghan et al., 2001; Graf et al., 1997; Grant et al., 1999); –0.2 W/m^2 (–0.07–0.6 W/m^2) for biomass burning aerosols (Myhre et al., 1998; Hobbs et al., 1997; Liousse et al., 1996; Ross et al., 1998); –0.10 W/m^2 (–0.03– –0.3 W/m^2) for fossil fuel organic carbon aerosols (Cooke et al., 1999; Myhre et al., 2001; Penner et al., 1998); +0.2 W/m^2 (+0.1–+0.4 W/m^2) for fossil fuel black carbon aerosols (Grant et al., 1999; Hansen et al., 1998; Penner et al., 1998) and –0.6–+0.4 W/m^2 for mineral dust aerosols (Hansen et al., 1998; Jacobson, 2001; Miller and Tegen, 1998; Sokolik and Toon, 1996; Tegen and Lacis, 1996). Exploratory studies on atmospheric radiation effects of mixed aerosols have also been carried out (Hobbs et al., 1997; Christopher and Zhang, 2004; Wang et al., 2013; Zhang et al., 2012).

A great deal of work on aerosol DRF, abbreviated as DRF, has been carried out in China. Chen et al. (2004) analysed the impact of aerosols on climate change over China and pointed out that the coupled increase of aerosol with economic development is considered the main reason for a decline in temperature in China. Mao and Li (2005) studied the aerosol radiative properties over China and retrieved aerosol optical properties from MODIS data. Sun and Liu (2008a, 2008b) have estimated over China the

effects of sulfate aerosols and black carbon (BC) on the East Asian summer monsoon and the results show that sulfate and black carbon aerosols produce a global average radiative forcing of –0.25 and 0.13 W/m^2, respectively. A simulation study of radiative forcing of organic carbon (OC) aerosols in China with RegCM3 model, showed the radiative forcing on top of the atmosphere to be negative between –0.1 and –0.5 W/m^2 (Su et al., 2010). Lu et al. (2011) analysed the influences of BC and OC aerosols on air temperature, and discovered that BC and OC aerosols cause a distinct increase in air temperature between 28°–30° N latitude versus a decrease between 35°–36.2°N in China.

The Pearl River Delta (latitude 21.5–24°N, longitude 112–115.5°E), located in south central Guangdong China (Figure 1), has experienced fast economic growth, population expansion and consequently severe aerosol pollution all year round. Anthropogenic aerosol generation has witnessed a dramatic increase in past several decades, with the rapid industrial development, vegetation reduction, and heavy traffic pressure. The yearly average aerosol type over PRD is shown in Table 1, proposed by Li et al. (2005), which has been proved to be suitable for Hong Kong and the adjacent areas of PRD. Dust-like, water-soluble, oceanic and soot aerosols make up the complicated aerosol types in the region, with the volume components of 0.13 ± 0.1, 0.7 ± 0.12, 0.15 ± 0.11 and 0.005 ± 0.004, respectively. Annual average aerosol optical thickness (AOT) over PRD region in 2011, derived from MODIS 10 km-resolution AOT products, was calculated about 0.53 (Figure 2). Therefore, regional study on aerosol DRF will play an important role in the study of climatic effects in the future.

Figure 1 Location and administrative boundary of the Pearl River Delta in Guangdong Province, China (21.5~24°N, 112~115.5°E) (see online version for colours)

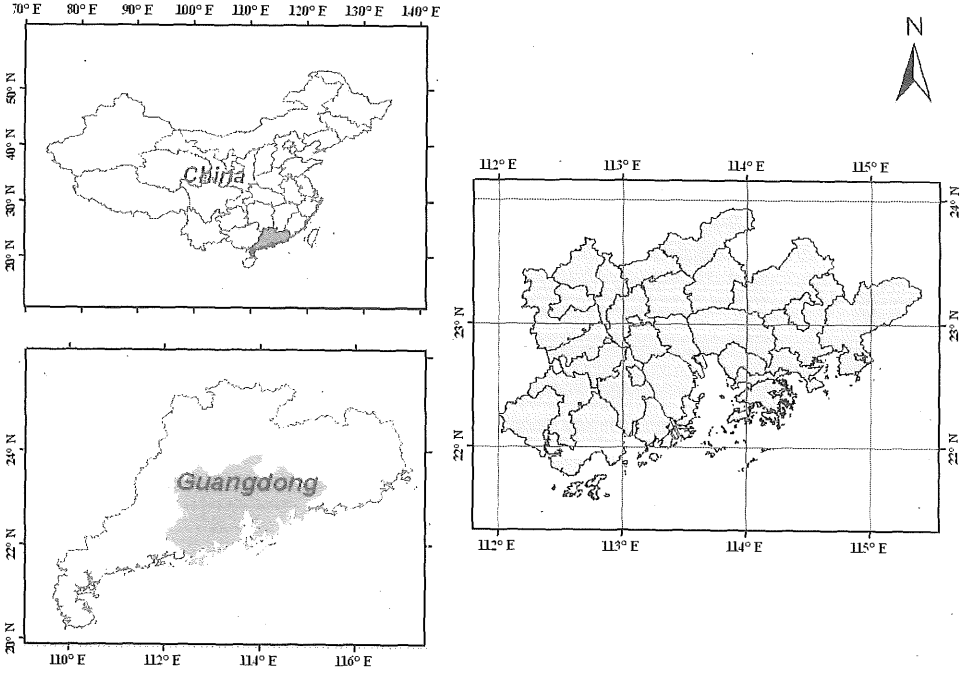

Table 1 The four basic components in the aerosol model

	Dust-like	*Water-soluble*	*Oceanic*	*Soot*
Volume component	0.13	0.7	0.15	0.005
Standard deviation	0.1	0.12	0.11	0.004

Source: Li et al. (2005)

Figure 2 Annual average AOT distribution map with 10 km-resolution over Pearl River Delta region in 2011 (see online version for colours)

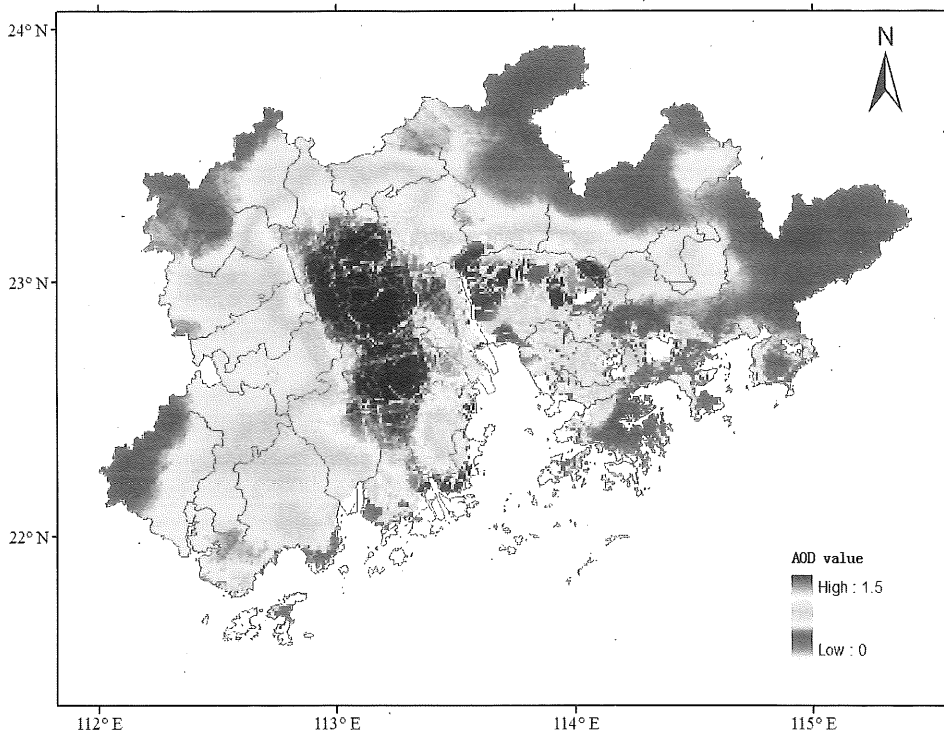

2 Methodology

2.1 Two-layer-single-wavelength model

Seinfeld and Pandis (1998) constructed a single thin layer aerosol ground surface radiation model illustrated in Figure 3. It shows an aerosol layer lying on top of a ground surface layer. The direct incident solar radiation beam impinges on the aerosol layer with radiative flux F_0. The model assumes a light beam perpendicular to the surface, i.e., at a solar zenith angle θ of 0° and an adiabatic temperature profile.

Figure 3 Two-layer-single-wavelength radiation model (a thin aerosol layer above the Earth's surface)

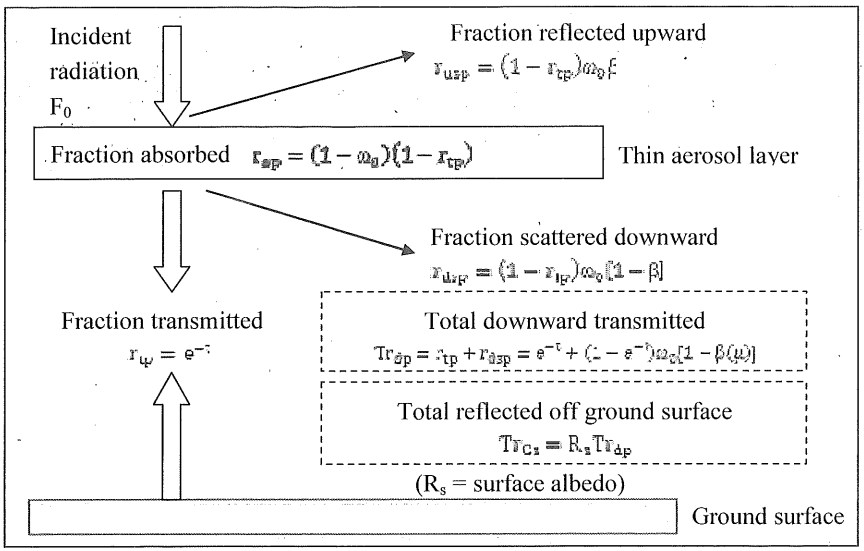

Source: Proposed by Seinfeld and Pandis (1998)

The fraction of the incident light transmitted through the aerosol layer is $r_{tp} = e^{-\tau}$, where τ is the optical depth of the layer, showing the vertical integral of particle extinction coefficient σ_{ep} over the layer. The fraction of the incident radiation reflected by the surface

$$Tr_{GS} = R_s Tr_{dp} = R_s \left(r_{tp} + r_{dsp} \right) \tag{1}$$

where R_s is the albedo of the underlying Earth's surface, r_{dsp} is the fraction of the radiation scattered downward. Some of the intensity $R_s Tr_{dp} F_0$, reflected upward by the ground surface into the aerosol layer, is backscattered, some is absorbed by the layer, and some is transmitted to the outer atmosphere. For these multiple radiative processing, the total upward flux is

$$\begin{aligned} F_r &= \left(r_{usp} + R_s Tr_{dp}^2 + R_s^2 Tr_{dp}^2 r_{usp} + \cdots \right) F_0 \\ &= \left[r_{usp} + R_s Tr_{dp}^2 \left(1 + R_s r_{usp} + R_s^2 r_{usp}^2 + R_s^3 r_{usp}^3 + \cdots \right) \right] F_0 \end{aligned} \tag{2}$$

where r_{usp} is the fraction reflected back to the atmosphere. With $R_s < 1$ and $r_{usp} < 1$, equation (4) simplifies to

$$F_r = \left(r_{usp} + \frac{R_s Tr_{dp}^2}{1 - R_s r_{usp}} \right) F_0 \tag{3}$$

In fact, even if totally devoid of aerosols, the atmosphere does not completely transmit the incident solar beam. Considering the atmosphere as a blanket overlaying the aerosol layer, the incident flux on the aerosol layer is $T_{atm} F_0$ instead of F_0. The change in outwards radiative flux due to the aerosol layer is the aerosol DRF ΔF_r:

$$\Delta F_r = F_{ar} - F_{a0} = \Delta R_p F_0 = T_{atm}^2 \left[\left(r_{usp} + \frac{R_s T r_{dp}^2}{1 - R_s r_{usp}} \right) - R_s \right] F_0 \quad (4)$$

where F_{ar} is upwards radiative flux when there exists aerosols, F_{a0} is upwards radiative flux when without aerosols and ΔR_p stands for quantity in square brackets. If $\Delta R_p > 0$, $\Delta F_r > 0$, then the net change in forcing is $-|\Delta F_r|$ and results in cooling effects. If ΔF_r on the other hand is smaller than 0, the climatic effect is warming. That is, aerosol DRF is the difference in radiative flux between aerosols (F_{ar}) and no aerosols (F_{a0}).

2.2 *Introduction of SBDART*

To calculate aerosol DRF in the Pearl River Delta region we did choose the Santa Barbara DISORT atmospheric radiative transfer (SBDART) program to study the effects of aerosols on top-of-atmosphere upwards radiant flux. SBDART is a FORTRAN computer code developed by the Earth Space Research Group of the Institute for computational Earth System Science at the University of California (Ricchiazzi et al., 1998). It analyses various radiative transfer problems in satellite remote sensing and atmospheric energy budget studies. Based on a collection of highly developed physical models, SBDART can be used to compute the intensity of scattered and emitted radiation at different heights and directions, and allows over 50 atmospheric layers and 20 radiation streams to enhance calculation accuracy.

To simulate the top-of-atmosphere and surface upwelling radiant flux with SBDART, three basic types of input are required:

1 solar geometry: latitude and longitude, date, time and spectral region

2 atmospheric profile: the concentration of water vapor, ozone and trace gases such as CO_2, CH_4 and NO_X, together with a surface albedo model to parameterise the spectral reflectivity of the surface, by choosing surface type or set the albedo to be a constant

3 aerosol parameters: aerosol types, altitude of stratospheric aerosol and AOT.

Outputs calculated by the model are total downward flux (W/m^2), total upward flux (W/m^2), direct downward flux (W/m^2), Net flux (W/m^2), and Heating rate (K/day). The model assumes no divergence of the heat moving upwards.

In our study, we first calculate the 24-hours flux up over asphalt and vegetation on the first day of each month in 2011, respectively, to make a clear comparison of seasonal variation of aerosol shortwave DRF on different underlying surfaces. We also estimated the average shortwave DRF and net radiation at different solar zenith angle and AOT to study their variations. The average AOT over PRD region in this model is set to 0.5, and the tropospheric aerosol types are set as urban and no aerosol in the model. The altitude is set as 10 km because it is the average height of the troposphere layer in middle or lower latitude regions. Table 2 lists the input parameters on January 1 over the PRD in our experiment.

Table 2 The input parameter for SBDART on January 1, 2011 for the Pearl River Delta

Solar geometry		
Lat. and lon.	*Date*	*Time*	*Spectral region (μm)*
23.1°N, 113.3°E	Jan. 1st	0–24 hour	0.25–4.00
Atmospheric profile		
Water vapor (g/cm^2)	Ozone (ATM-cm)	CO_2 (ppm)
1	0.35	360
CH_4 (ppm)	NO_X (ppm)	Surface albedo model
1.74	0.32	Vegetation/urban asphalt
Aerosol parameters		
Background aerosol type	Altitude (km)	AOT
Rural/urban/no aerosol	10	0.5

3 Calculation of direct shortwave radiative forcing over the Pearl River Delta

Figures 4 and 5 show the hourly variation of top-of-atmosphere shortwave radiant flux F_{ar} (AOT = 0.5) and F_{a0} (AOT = 0) on the first day of each month over the Pearl River Delta region with the underlying surface being vegetation and urban asphalt, respectively. The blue curve in these figures indicates the daily evolution of F_{a0} for a tropospheric background without aerosol, the red curve the evolution of F_{ar} with an AOT set at 0.5. The aerosol types are assumed the same in the model to avoid the difference impact on the results. Considering the size of the study area, this assumption is acceptable and has no obvious influence on the results. The curves vary in height, a measure of the flux intensity, and width indicative of the variation in flux during the daily cycle. When the peak intensity of the red curve is larger than that of the blue curve, cooling occurs; when the peak intensity of the blue curve is larger, warming occurs.

Thus, inspection of Figure 4 shows that with a vegetation substrate and an AOT of 0.5, $\Delta F_r = F_{ar} - F_{a0}$ is positive between January and March indicative of cooling, ΔF_r reaching 16.94 W/m^2, 13.05 W/m^2 and 8.03 W/m^2, respectively. Cooling with decreasing intensity continues on April 1st except from 3:00 to 7:00 Greenwich mean time (GMT, 11:00 am to 15:00 pm locally) when ΔF_r is –6.06 W/m^2, indicative of warming. In May and June, warming continued to increase along with lengthening of duration. Warming reached its apogee in July with a peak value of 8.58 W/m^2, between 2:00 and 7:30 GMT (10:00 am to 15:30 pm locally). After July the warming intensity gradually decreased as well as the number of daily hours. Cooling took over again in November and ΔFr increased up to 16.42 W/m^2 in December.

Figure 4 The variation of top-of-atmosphere upwelling radiant flux F_{ar} and F_{a0} on the first day of each month over the Pearl River Delta region with vegetation as underlying surface (see online version for colours)

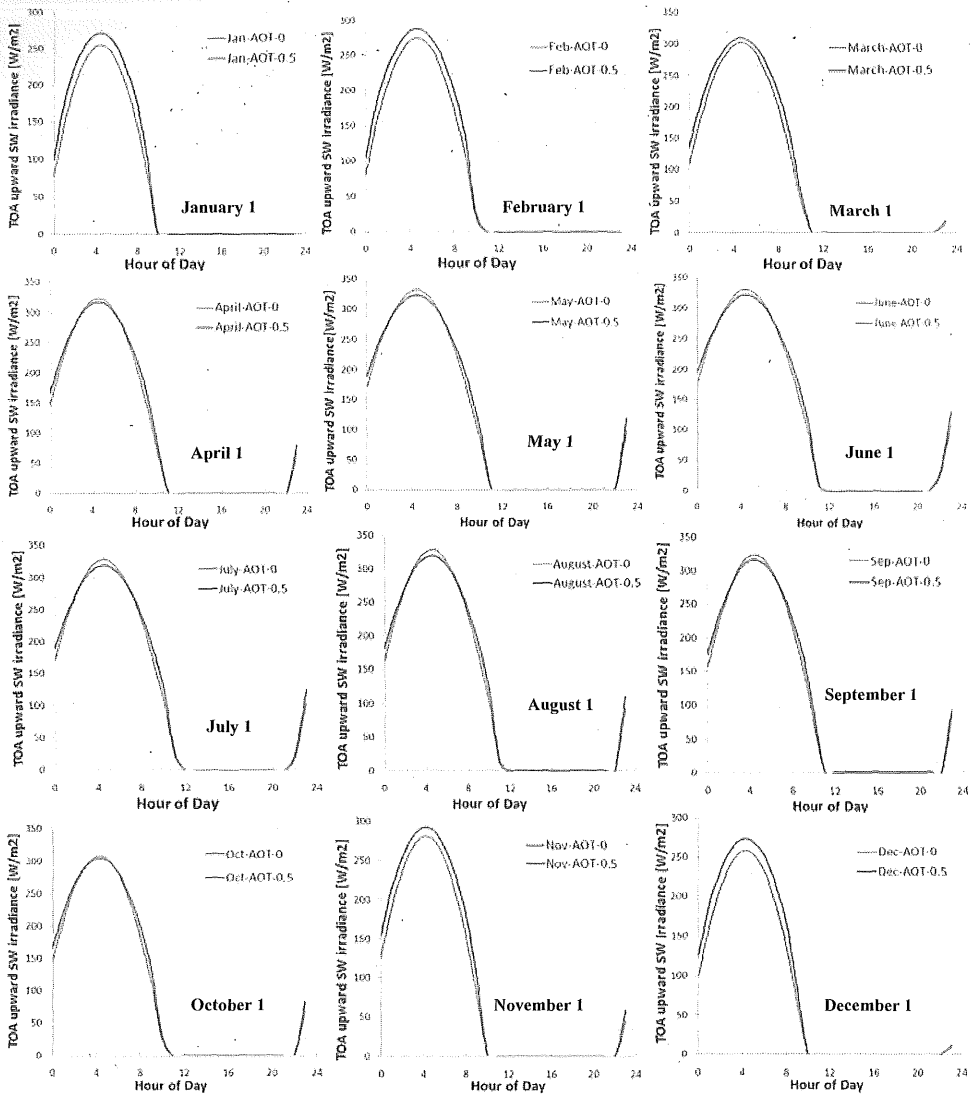

Note: The hour represents the Greenwich mean time, about eight hours earlier than the local time.

Figure 5 show that, in urban asphalt areas with an AOT set at 0.5, $\Delta F_r = F_{ar} - F_{a0}$ was 33.56 W/m^2 in January indicative of cooling. However in contrast to the case with a vegetation substrate, already on February 1 DRF becomes negative (–10.59 W/m^2) between 2:30 to 7:00 GMT indicative of warming. Warming continued to increase between March to June in intensity as well as hours per day. Warming was highest in July, with a peak value of 18.99 W/m^2 between 0 and 8:00 GMT. From August to October the warming gradually decreased in intensity as well duration. Cooling took over

in November and with December, ΔF_r becoming positive with a value of 11.19 W/m^2 and 16.21 W/m^2, respectively.

Figure 5 The variation of top-of-atmosphere upwelling radiant flux F_{ar} and F_{a0} on the first day of each month over PRD region with urban asphalt as the underlying surface (see online version for colours)

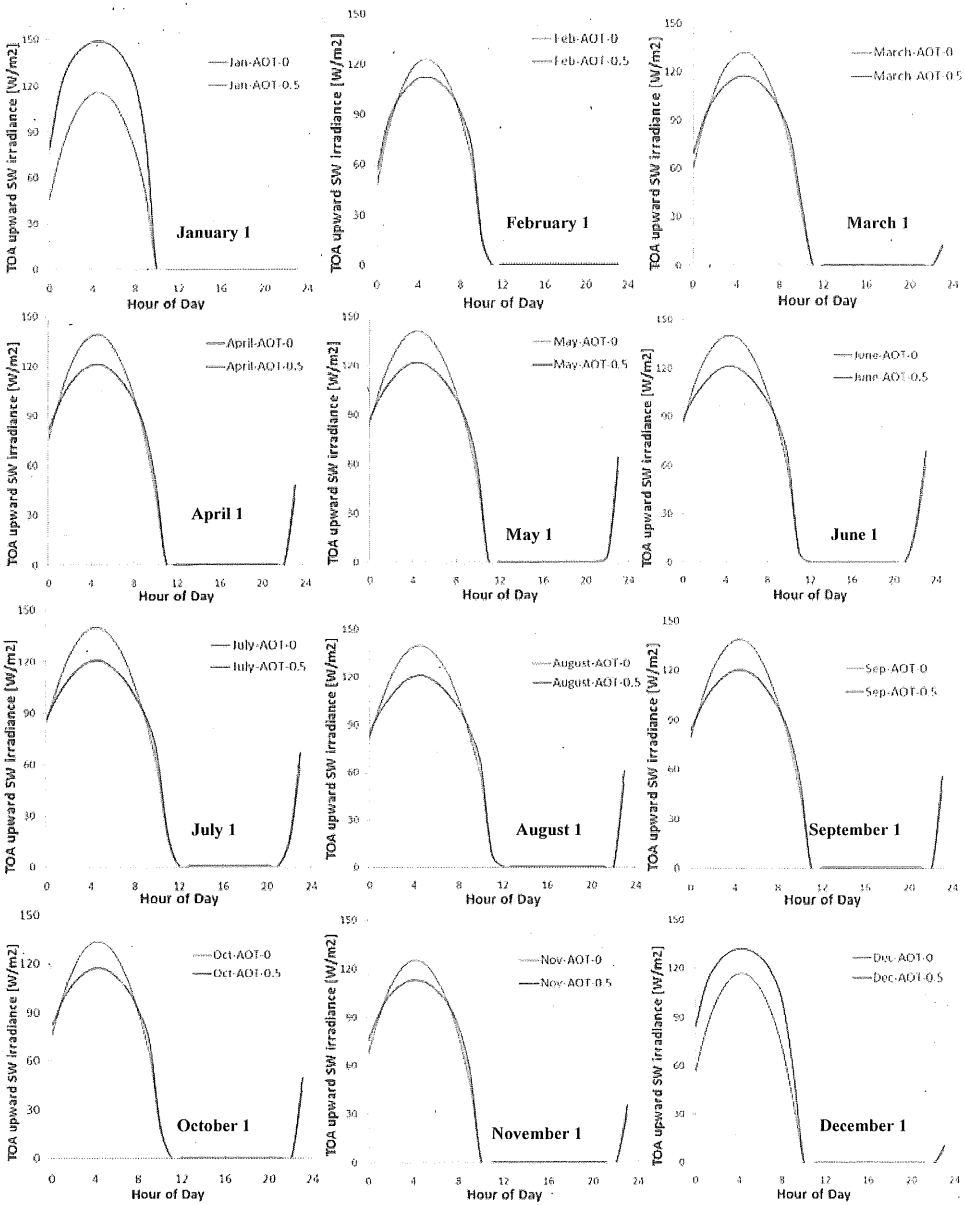

Note: The hour represents the Greenwich mean time, about eight hours earlier than the local time.

As discussed above, Figures 4 and 5 indicate cooling in winter (November, December and January) and warming during the other seasons in the Pearl River Delta. Note that the effect of aerosol direct shortwave radiative forcing is much stronger in the urban area where asphalt predominates than that in the rural area where vegetation prevails.

4 Average DRF and shortwave net radiation flux over the Pearl River Delta

Net radiation is the balance between incoming solar energy and outgoing energy from the Earth. It is the total energy that influences climate and provides important information about Earth's energy budget. For discovering the variation trends, we also calculated the average shortwave DRF and NR at different solar zenith angle and AOT values in the Pearl River Delta in year 2011 through SBDART.

Figure 6 Variation of average upwards radiant flux in Pearl River Delta with AOT: SZA in each figure is (a) 0°, (b) 20°, (c) 40°, (d) 60° and (e) 80° (see online version for colours)

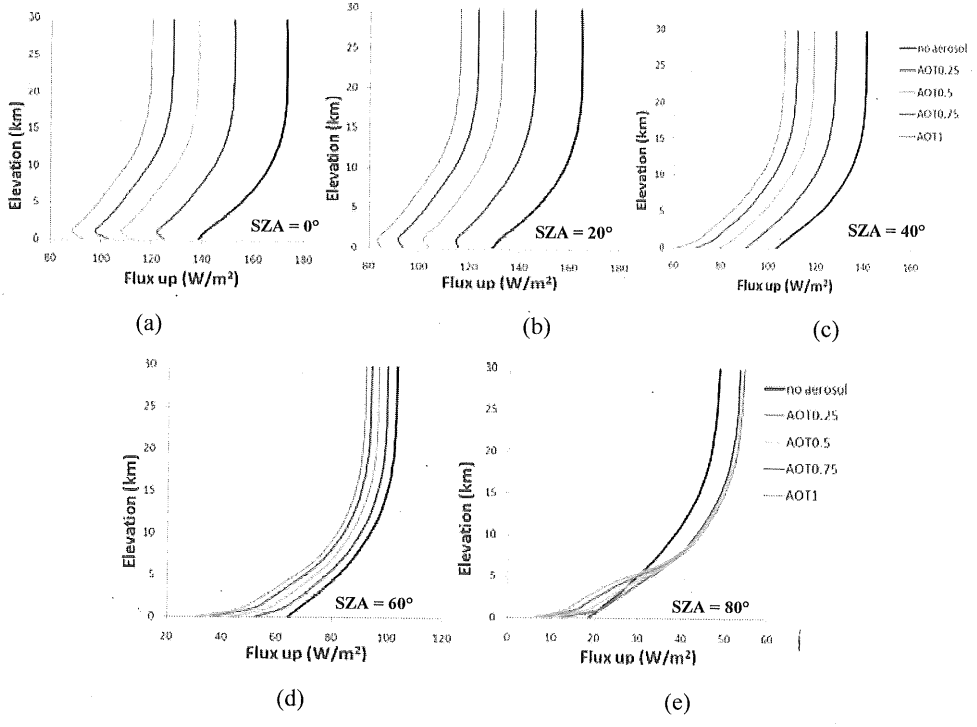

The variation of upwards radiant flux with AOT at different solar zenith angle is shown in Figure 6. Note that:

1 the upwelling radiant flux decreases with the increase of solar zenith angle

2 when SZA is 0°, 20°, 40° and 60°, the upwelling radiant flux decreases with an increasing AOT, but for SZA = 80°, the decrease only occurs below 5 km

3 with increasing elevation, upwelling radiant flux increases

4 when SZA is 0°, 20°, 40° and 60°, aerosol DRF $\Delta F_r = F_{ar} - F_{a0}$ is negative indicative of warming. In addition, the warming intensity increases with increasing AOT while it decreases with increasing SZA

5 when SZA is 80°, ΔF_r is positive, i.e., cooling, the intensity increasing with increasing AOT.

Figure 7 displays the variation of shortwave net flux along with SZA and AOT over the Pearl River Delta. It can be inferred from this figure that:

1 The shortwave net flux decreases with increasing AOT, meaning that aerosol can effectively reduce the shortwave solar radiation energy received by the earth.

2 The shortwave net flux increases with increasing elevation, because atmospheric layer on top of the aerosol layer also absorbs some degree of solar energy.

3 When SZA is 0°, 20°, 40° and 60°, with the increase of AOT, the shortwave net flux gradually decreases near the ground and then increase above about 5 km. As a consequence, the difference between net flux in the upper atmosphere and that on the surface increases with the increase of AOT. This difference is exactly the radiation energy absorbed and used by the atmosphere.

4 When SZA is 80°, there is no positive relationship between the net radiation difference and AOT.

Figure 7 Variation of average net flux in Pearl River Delta with AOT: SZA in each figure is (a) 0°, (b) 20°, (c) 40°, (d) 60° and (e) 80° (see online version for colours)

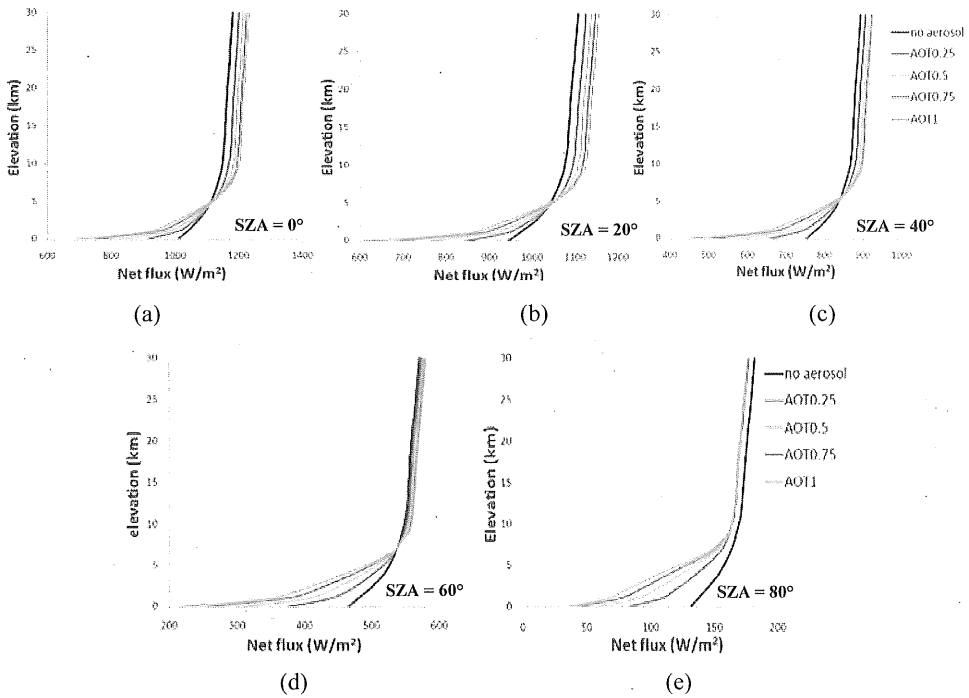

5 Conclusions

This study used the SBDART model to calculate and analyse the annual aerosol shortwave DRF and net flux over the Pearl River Delta region. In general, DRF in this region is affected by underlying surface type and solar zenith angle.

Comparison of aerosol shortwave DRF between vegetation and urban asphalt in Pearl River Delta reveals some differences. In January and February ΔF_r was positive for vegetation, indicative of cooling with a peak at January 1st of 16.94 W/m^2; till July warming increased with a peak at 8.58 W/m^2. For the urban asphalt area, the DRF of January indicated cooling, reaching up to 33.56 W/m^2; the climate warms in February with a maximum of 18.98 W/m^2 in July. Hence, the warming intensity over urban asphalt surface is much greater than that over vegetation.

After computing the shortwave average albedo from the satellite data, we also estimated the average shortwave DRF and net radiation over the Pearl River Delta by SBDART. Our results show that at a solar zenith angle of 0°, 20°, 40° and 60°, shortwave DRF induces warming which increases with increasing AOT and decreases with increasing SZA; When SZA is 80°,DRF induces cooling the more so with increasing AOT. Additionally, shortwave net flux tracks with a decrease in AOT at low elevations. This relationship weakens with increasing elevation and turns positive at about 5 km.

Acknowledgements

The China 863 Program (2006AA06A306) and Guangdong NSF (S2013010014097) are acknowledged for financial supports. We also thank the Institute for Computational Earth System Science, University of California, for the SBDART model. Prof. Bernard de Jong of Utrecht University is greatly acknowledged for his help to improve the English of this manuscript. This is contribution No. SKLOG2013A01 from SKLOG and No. IS-2141 from GIGCAS.

References

Alam, K., Trautmann, T. and Blaschke, T. (2011) 'Aerosol optical properties and radiative forcing over mega-city Karachi', *Atmospheric Research*, Vol. 101, No. 3, pp.773–782.

Albrecht, B.A. (1989) 'Aerosols, cloud microphysics, and fractional cloudiness', *Science*, Vol. 245, No. 4923, pp.1227–1230.

Carlson, T.N., Capehart, W.J. and Gillies, R.R. (1995) 'A new look at the simplified method for remote-sensing of daily evapotranspiration', *Remote Sensing of Environmeng*, Vol. 54, No. 2, pp.161–167.

Chen, L.X., Zhou, X.J. and Li, W.L. (2004) 'Characteristics of the climate change and its formation mechanism in China in last 80 years', *Acta Meteorologica Sinica* (Chinese), Vol. 62, No. 5, pp.634–646.

Christopher, S.A. and Zhang, J. (2004) 'Cloud-free shortwave aerosol radiative effect over oceans: strategies for identifying anthropogenic forcing from Terra satellite measurements', *Geophysical Research Letters*, Vol. 31, No. 18, pp.1–4, doi: 10.1029/2004GL020510.

Cooke, W.F., Liousse, C., Cachier, H. and Feichter, J. (1999) 'Construction of a 1 × 1 fossil fuel emission data set for carbonaceous aerosol and implementation and radiative impact in the ECHAM4 model', *Journal of Geophysical Research Atmosphere*, Vol. 104, No. D18, pp.22137–22162.

El-Metwally, M., Alfaro, S.C., Wahab, M.M., Favez, O., Mohamed, Z. and Chatenet, B. (2011) 'Aerosol properties and associated radiative effects over Cairo (Egypt)', *Atmospheric Research*, Vol. 99, No. 2, pp.263–276.

Gao, X., Lin, Y.H. and Zhao, Z.C. (2003) 'Modelling the effects of anthropogenic sulfate in climate change by using a regional climate model', *Journal of Tropical Meteorology* (Chinese), Vol. 19, No. 2, pp.169–176.

Ghan, S.J., Easter, R.C., Chapman, E.G., Abdul-Razzak, H., Zhang, Y., Leung, L.R., Laulainen, N.S., Saylor, R.D. and Zaveri, R.A. (2001) 'A physically based estimate of radiative forcing by anthropogenic sulfate aerosol', *Journal of Geophysical Research Atmosphere*, Vol. 106, No. D6, pp.5279–5293.

Graf, H.F., Feichter, J. and Langmann, B. (1997) 'Volcanic sulfur emissions: estimates of source strength and its contribution to the global sulfate distribution', *Journal of Geophysical Research Atmosphere*, Vol. 102, No. D9, pp.10727–10738.

Grant, K.E., Chuang, C.C., Grossman, A.S. and Penner, J.E. (1999) 'Modeling the spectral optical properties of ammonium sulfate and biomass burning aerosols: parameterization of relative humidity effects and model results', *Atmospheric Environment*, Vol. 33, No. 17, pp.2603–2620.

Hansen, J.E., Sato, M., Lacis, A., Ruedy, R., Tegen, I. and Matthews, E. (1998) 'Climate forcings in the industrial era', *Proceedings of the National Academy of Sciences of the USA*, Vol. 95, No. 22, pp.12753–12758.

Hobbs, P.V., Reid, J.S., Kotchenruther, R.A., Ferek, R.J. and Weiss, R. (1997) 'Direct radiative forcing by smoke from biomass burning', *Science*, Vol. 275, No. 5307, pp.1777–1778.

IPCC (2007) *Climate Change 2007: The Physical Science Basis: Contribution of Working Group II to the Fourth Assessment Report of the Intergovernmental Panel on Climate Change*, Cambridge University Press, Cambridge.

Jacobson, M.Z. (2001) 'Global direct radiative forcing due to multicomponent anthropogenic and natural aerosols', *Journal of Geophysical Research Atmosphere*, Vol. 106, No. D2, pp.1551–1568.

Kaufman, Y.J. and Fraser, R.S. (1997) 'The effect of smoke particles on clouds and climate forcing', *Science*, Vol. 277, No. 5332, pp.1636–1639.

Kaufman, Y.J. and Koren, I. (2006) 'Smoke and pollution aerosol effect on cloud cover', *Science*, Vol. 313, No. 5787, pp.655–658.

Kim, S.W., Choi, I.J. and Yoon, S.C. (2010) 'A multi-year analysis of clear-sky aerosol optical properties and direct radiative forcing at Gosan, Korea (2001–2008)', *Atmospheric Research*, Vol. 95, No. 2, pp.279–287.

Lau, K.M. and Kim, K.M. (2006) 'Observational relationships between aerosol and Asian monsoon rainfall, and circulation', *Geophysical Research Letters*, Vol. 33, No. L21810, pp.1–5, doi: 10.1029/2006GL027546.

Li, C.C., Mao, J.T. and Lau, A.K.H. (2005) 'Remote sensing of high spatial resolution aerosol optical depth with MODIS data over Hong Kong', *Chinese Journal of Atmospheric Sciences*, Vol. 29, No. 3, pp.335–342.

Li, Z.Q., Xia, X.G., Cribb, M., Mi, W., Holben, B., Wang, P.C., Chen, H.B., Tsay, S.C., Eck, T.F., Zhao, F.S., Dutton, E.G. and Dickerson, R.E. (2007) 'Aerosol optical properties and their radiative effects in northern China', *Journal of Geophysical Research Atmosphere*, Vol. 112, No. D22, pp.1–11, doi: 10.1029/2006JD007382..

Liousse, C., Penner, J.E., Chuang, C., Walton, J.J., Eddleman, H. and Cachier, H. (1996) 'A global three-dimensional model study of carbonaceous aerosols', *Journal of Geophysical Research Atmosphere*, Vol. 101, No. D14, pp.19411–19432.

Lu, P., Dong, Z.B. and Zhang, K.C. (2011) 'Numerical simulation effect of black carbon and organic carbon aerosols on atmospheric temperature in China', *Journal of Desert Research* (Chinese), Vol. 31, No. 2, pp.500–504.

Mao, J.T. and Li, C.C. (2005) 'Observation study of aerosol radiative properties over China', *Acta Meteorologica Sinica* (Chinese), Vol. 63, No. 5, pp.622–635.

Miller, R.L. and Tegen, I. (1998) 'Climate response to soil dust aerosols', *Journal of Climate*, Vol. 11, No. 12, pp.3247–3267.

Myhre, G., Myhre, A. and Stordal, F. (2001) 'Historical evolution of radiative forcing of climate', *Atmospheric Environment*, Vol. 35, No. 13, pp.2361–2373.

Myhre, G., Stordal, F., Restad, K. and Isaksen, I.S. (1998) 'Estimation of the direct radiative forcing due to sulfate and soot aerosols', *Tellus B*, Vol. 50, No. 5, pp.463–477.

Penner, J.E., Bergmann, D.J., Walton, J.J., Kinnison, D., Prather, M.J., Rotman, D., Price, C., Pickering, K.E. and Baughcum, S.L. (1998) 'An evaluation of upper troposphere NOx with two models', *Journal of Geophysical Research Atmosphere*, Vol. 103, No. D17, pp.22097–22113.

Penner, J.E., Charlson, R.J., Schwartz, S.E., Hales, J.M., Laulainen, N.S., Travis, L., Leifer, R., Novakov, T., Ogren, J. and Radke, L.F. (1994) 'Quantifying and minimizing uncertainty of climate forcing by anthropogenic aerosols', *Bulletin of the American Meteorological Society*, Vol. 75, No. 3, pp.375–400.

Penner, J.E., Chuang, C.C. and Grant, K. (1998) 'Climate forcing by carbonaceous and sulfate aerosols', *Climate Dynamics*, Vol. 14, No. 12, pp.839–851.

Pincus, R. and Baker, M.B. (1994) 'Effect of precipitation on the albedo susceptibility of clouds in the marine boundary-layer', *Nature*, Vol. 372, No. 6503, pp.250–252.

Reddy, M.S., Boucher, O., Venkataraman, C., Verma, S., Leon, J.F., Bellouin, N. and Pham, M. (2004) 'General circulation model estimates of aerosol transport and radiative forcing during the Indian Ocean experiment', *Journal of Geophysical Research Atmosphere*, Vol. 109, No. D16205, pp.1–15, doi: 10.1029/2004JD004557.

Ricchiazzi, P., Yang, S.R., Gautier, C. and Sowle, D. (1998) 'SBDART: a research and teaching software tool for plane-parallel radiative transfer in the Earth's atmosphere', *Bulletin of the American Meteorological Society*, Vol. 79, No. 10, pp.2101–2114.

Ross, J.L., Hobbs, P.V. and Holben, B. (1998) 'Radiative characteristics of regional hazes dominated by smoke from biomass burning in Brazil: closure tests and direct radiative forcing', *Journal of Geophysical Research Atmosphere*, Vol. 103, No. D24, pp.31925–31941.

Seinfeld, J.H. and Pandis, S.N. (1998). *Atmospheric Chemistry and Physics: From Air Pollution to Climate Change*, John Wiley & Sons Inc., New York.

Sokolik, I.N. and Toon, O.B. (1996) 'Direct radiative forcing by anthropogenic airborne mineral aerosols', *Journal of Aerosol Science*, Vol. 27, No. Supple. 1, pp.11–12.

Su, X., Wang, H.J. and Zhou, L. (2010) 'A simulation study on temporal and spatial distribution characteristics and radiative forcing of organic carbon aerosols in China', *Journal of Tropical Meteorology* (Chinese), Vol. 26, No. 6, pp.765–772.

Sun, J.R. and Liu, Y. (2008a) 'Possible effect of aerosols over China on East Asian summer monsoon (I): sulfate aerosols', *Advances in Climate Change Research* (Chinese), Vol. 4, No. 2, pp.111–116.

Sun, J.R. and Liu, Y. (2008b) 'Possible effects of aerosols over China on East Asian summer monsoon (I): black carbon and its joint effects with sulfate aerosols', *Advances in Climate Change Research* (Chinese), Vol. 4, No. 3, pp.161–166.

Tegen, I. and Lacis, A.A. (1996) 'Modeling of particle size distribution and its influence on the radiative properties of mineral dust aerosol', *Journal of Geophysical Research Atmosphere*, Vol. 101, No. D14, pp.19237–19244.

Twomey, S. (1974) 'Pollution and the planetary albedo', *Atmospheric Environment*, Vol. 8, No. 12, pp.1251–1256.

Wang, Z.L., Zhang, H., Jing, X.W. and Wei, X.D. (2013) 'Effect of non-spherical dust aerosol on its direct radiative forcing', *Atmospheric Research*, Vol. 120–121, pp.112–126.

Wu, D. (2003) 'A review and outlook on the aerosol study over South China', *Journal of Tropical Meteorology* (Chinese), Vol. 19, No. Suppl., pp.145–151.

Zhang, H., Shen, Z., Wei, X., Zhang, M. and Li, Z. (2012) 'Comparison of optical properties of nitrate and sulfate aerosol and the direct radiative forcing due to nitrate in China', *Atmospheric Research*, Vol. 113, No. 5, pp.113–125.

Zhang, X.Y., Wang, Y.Q., Niu, T., Zhang, X.C., Gong, S.L., Zhang, Y.M. and Sun, J.Y. (2012) 'Atmospheric aerosol compositions in China: spatial/temporal variability, chemical signature, regional haze distribution and comparisons with global aerosols', *Atmospheric Chemistry and Physics*, Vol. 12, No. 2, pp.779–799.